JOURNAL OF MATERIALS SCIENCE 39 (2004) 3089–3094

Measurement of yield strength of thin metal film

FEI WANG, KEWEI XU*
State-Key Laboratory for Mechanical Behavior of Materials, Xian Jiaotong University, Xian 710049, People's Republic of China
E-mail: kwxu@mail.xjtu.edu.cn

Based on measurement of the load-depth curve in nanoindentation, the yield strength of thin metal film on Si substrate can be determined with the model of finite element analysis. An example is given of thin Cu film and the result shows that the yield strength thus determined can eventually reflect changes of processing condition both in deposition and in post-treatment. The yield strength and its variation can be explained in terms of grain orientation and grain size. © *2004 Kluwer Academic Publishers*

1. Introduction

Mechanical properties are main researches for a structural material. With the application of film-coated materials or devices in microelectronics, optics and so on, it becomes more and more apparent and realized that the mechanical properties are essential and closely related to performance and reliability of film-coated devices. Although mechanical measurements of thin film are difficult and few methods are available, great efforts have been made in the past in exploring theoretical and experimental techniques, such as uni-axial tension [1, 2], bulge test [3, 4], micro-beam deflection [5], nanoindentation [6], wafer curvature in thermal cycle [7–9], and X-ray diffraction [10]. Among them the nanoindentation technique is a powerful tool in measurement of elastic modulus and micro-hardness [11–14], and has been used to calculate the yield strength of thin metal film [15]. It is believed that the flow properties and creep properties of thin metal film will be eventually taken into consideration in the service of film-coated devices, and more abnormal phenomena will be highlighted in this field.

It was found that the yield strength of pure Al film on Si substrate, measured with a substrate curvature technique, was higher than that of free-standing Al-1%Si film measured with bulge testing method [4, 13]. Bader and Shute measured the yield strength of Al film by X-ray diffraction according to differences of thermal expansion coefficient between substrate and film [16, 17], although it was difficult to get the yield strength at room temperature because of required changes in temperature. Li and his co-workers recently showed that, for identical thickness of Al films on Si substrates, the yield strength of the Al film with a SiO_2 passivated layer was higher than that of the un-passivated film [18]. Other researchers preferred to get the flow properties by calculations, and then compared them with experimental results. Bhattacharya and Nix [7] have explored successfully an empirical formula for hardness and elastic properties in nanoindentation with a cortical indenter.

In the present research, dimensional analysis was applied to derive the nanoindentation responses of bulk material and film/substrate composite using a Berkovich indenter. Using the derived expressions associated with finite element calculation, a relationship between the mechanical properties and the nanoindentation responses of the tested material was obtained. For thin metal films deposited on hard substrate, such as silicon or alumina, a method could be eventually established for determining the yield strength of thin metal film from nanoindentation loading curve. Using this model in which the Berkovich bluntness has been modified, the yielding strength of Cu thin films and its variation under different processing conditions are calculated and discussed.

2. Dimensional analyses

2.1. Nanoindentation of bulk material

The load-depth curve of an ideal Berkovich indenter as shown in Fig. 1 can be simulated by a power function [15],

$$P = P_m(h/h_m)^x \tag{1}$$

where h_m the highest depth of nanoindentation and P_m is the maximum load of nanoindentation, and x is an exponent of loading function.

The P_m and x in Equation 1 can be expressed as a function of mechanical properties of tested material and the maximum depth of nanoindentation.

$$\begin{aligned} P_m &= P_m(\sigma_y, n, E, h_m, \nu), \\ x &= x(\sigma_y, n, E, h_m, \nu) \end{aligned} \tag{2}$$

where σ_y, n, E, h_m, and ν are yield strength, hardening exponent, elastic modulus, maximum depth and

*Author to whom all correspondence should be addressed.

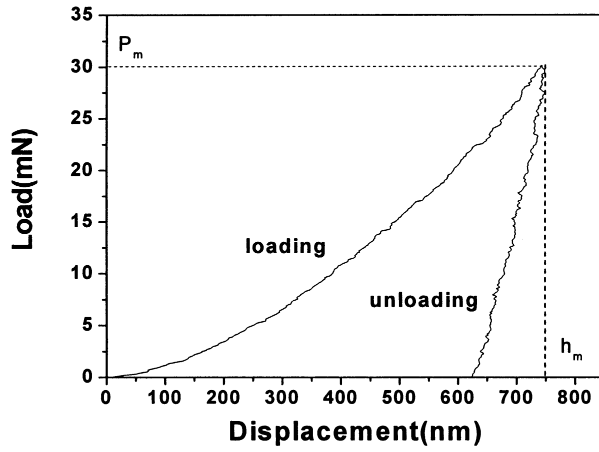

Figure 1 Typical nanoindentation curve.

Passion's ratio, respectively, of the tested material. According to dimensionally analytical Π theorem, it can be judged that only two of them are independent among the five parameters in Equation 2. If E and h_m are basic parameters, the other parameters can be expressed as

$$\frac{P_m}{Eh_m^2} = \Phi\left(\frac{\sigma_y}{E}, n, \nu\right), \quad x = \Psi\left(\frac{\sigma_y}{E}, n, \nu\right) \tag{3}$$

Assuming the Poisson's ratio is constant of 0.3, its effect in Equation 4 can be neglected. And the non-dimension function of the load-depth curve on bulk material with an ideal Berkovich indenter is obtained,

$$\frac{P_m}{Eh_m^2} = \Phi\left(\frac{\sigma_y}{E}, n\right), \quad x = \Psi\left(\frac{\sigma_y}{E}, n\right) \tag{4}$$

Generally, the tip of the diamond indenter will ineluctably be blunted because of wearing in nanoindentation, and the deviation thus produced must be modified. For the nanoindentation of bulk material with blunted Berkovich indenter, Δh was usually defined as an absolute bluntness, thus the P_{mbb} and X_{bb} can be described as a function of mechanical properties of material and the maximum depth of nanoindentation,

$$\begin{aligned} P_{mbb} &= P_{mbb}(\sigma_y, n, E, h_m, \Delta h), \\ x_{bb} &= x_{bb}(\sigma_y, n, E, h_m, \Delta h) \end{aligned} \tag{5}$$

Equation 4 is then changed to:

$$\frac{P_{mbb}}{Eh_m^2} = \Phi\left(\frac{\sigma_y}{E}, n, \frac{\Delta h}{h_m}\right), \quad x_{bb} = \Psi\left(\frac{\sigma_y}{E}, n, \frac{\Delta h}{h_m}\right) \tag{6}$$

where $\Delta h/h_m$ is relative bluntness of Berkovich indenter in Equation 6.

2.2. Nanoindentation of film/substrate material

For nanoindentation of film/substrate material with the ideal Berkovich indenter, if P_{mca} and x_{ca} is maximum load and fitting exponent of load curve of nanoindentation, respectively, the Equation 2 can be changed to:

$$\begin{aligned} P_{mca} &= P_{mca}(\sigma_f, n_f, E_f, \sigma_s, n_s, E_s, h_m, t_f), \\ x_{ca} &= x_{ca}(\sigma_f, n_f, E_f, \sigma_s, n_s, E_s, h_m, t_f) \end{aligned} \tag{7}$$

where σ_f, σ_s, n_f, n_s, E_f, and E_s are yield strength, hardening index and elastic modulus of the film and the substrate, respectively, and t_f is the thickness of film. Considering the bluntness, the P_{mca} and x_{ca} can be expressed as

$$\begin{aligned} P_{mca} &= P_{mca}(\sigma_f, n_f, E_f, \sigma_s, n_s, E_s, h_m, t_f, \Delta h), \\ x_{ca} &= x_{ca}(\sigma_f, n_f, E_f, \sigma_s, n_s, E_s, h_m, t_f, \Delta h) \end{aligned} \tag{8}$$

The non-dimension of the function of maximum load-depth curve of film/substrate material with the blunted Berkovich indenter can be expressed based on the method for bulk material,

$$\begin{aligned} \frac{P_{mcb}}{E_s h_m^2} &= \Phi_{cb}\left(\frac{\sigma_f}{E_s}, n_f, \frac{E_f}{E_s}, \frac{\Delta h}{h_m}\right), \\ x_{cb} &= \Psi_{cb}\left(\frac{\sigma_f}{E_s}, n_f, \frac{E_f}{E_s}, \frac{\Delta h}{h_m}\right) \end{aligned} \tag{9}$$

2.3. Calculation of yield strength

For nanoindentation of the surface of film with the ideal Berkovich indenter, the non-dimensional function of maximum load-depth curve is [15],

$$\begin{aligned} \frac{P_{mca}}{E_s h_m^2} &= \Phi_{ca}\left(\frac{\sigma_{yf}}{E_s}, n_f, \frac{E_f}{E_s}\right), \\ x_{ca} &= \Psi_{ca}\left(\frac{\sigma_{yf}}{E_s}, n_f, \frac{E_f}{E_s}\right) \end{aligned} \tag{10}$$

and the corresponding specific function is

$$P_{mca}/E_s h_m^2 = e^{\alpha(n)}(\sigma_y/E_s)^{\beta(n)}(E_f/E_s)^{\gamma(n)} \tag{11}$$

where α, β and γ are constants relative to the hardening index n, and can be expressed with the Equation 12,

$$\theta(n) = \theta_1 + \theta_2 n \tag{12}$$

As discussed above, the deviation due to the bluntness of indenter should be modified. For nanoindentation of film/substrate material with the blunted indenter, the non-dimensional function of maximum load-depth curve can be expressed as

$$\begin{aligned} \frac{P_m}{E_s h_m^2} &= \Phi\left(\frac{\sigma_y}{E_s}, n, \frac{E_f}{E_s}, r\right) \\ x &= \Psi\left(\frac{\sigma_y}{E_s}, n, \frac{E_f}{E_s}, r\right) \end{aligned} \tag{13}$$

Through numerical analysis, the ratio of $P_m/E_s h_m^2$ between the blunted indenter and the ideal indenter is

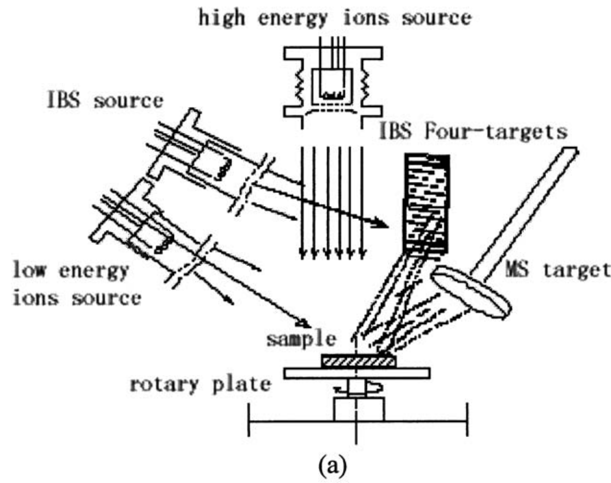

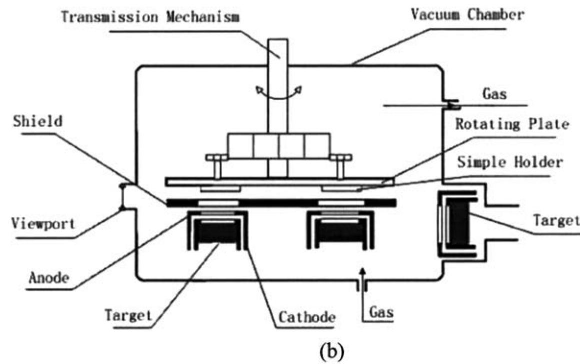

Figure 2 Schematics of vapor deposition: (a) A schematic co-sputtering of ion bean enhance deposition. (b) JGP560V ultra-vacuum magnetron sputtering.

a function of r and n that can be expressed with K, and the value of K depend on r and n.

When the blunted Berkovich indenter penetrates the surface of film, which is deposited on a rigidity substrate, the non-dimensional function of the max loading and the fitting exponent of load curve can be established based on Equation 11,

$$P_{\mathrm{mcb}}/E_{\mathrm{s}}h_{\mathrm{m}}^{2} = k(r, n_{\mathrm{f}})e^{\alpha(\mathrm{n})}(\sigma_{\mathrm{f}}/E_{\mathrm{s}})^{\beta(\mathrm{n})}(E_{\mathrm{f}}/E_{\mathrm{s}})^{\gamma(\mathrm{n})}$$

The fitting exponent x which is calculated from the nanoindentation loading curve, and is independent of $\sigma_{\mathrm{y}}/E_{\mathrm{s}}$ and dependent on n and r, can be expressed as

$$x_{\mathrm{cb}} = L_0(r) + L_1(r)n_{\mathrm{f}} + L_2(r)n_{\mathrm{f}}^2 \quad (14)$$

where $L_0(r)$, $L_1(r)$ and $L_2(r)$ are constants which can be obtained from the loading curve of nanoindentation. Thus the hardening index of the thin film can be calculated with the expression,

$$n = \left(\sqrt{L_1^2 + 4L_2(x - L_1) - L_1}\right)/(2L_2) \quad (15)$$

Based on the values of n, α, β and γ which are calculated with Equation 12, and the value of K, the yield strength of the thin film can be calculated with the Equation 16,

$$\sigma = E_{\mathrm{s}}\left[\left(P\big/\left(E_{\mathrm{s}}h_{\mathrm{m}}^2\right)\right)/(Ke^{\alpha}(E_{\mathrm{f}}/E_{\mathrm{s}})^{\gamma})\right]^{1/\beta} \quad (16)$$

3. Experimental

3.1. Prepared samples

Cu films were deposited with two techniques, the equipment of which is schematically shown in Fig. 2. For magnetron sputtering, only the biasing was changed, while for ion beam enhanced deposition (IBED) samples annealing in Ar and H_2 was adopted. The annealing temperature was kept at 100, 200 and 300°C for 1 h respectively.

Before deposition, the silicon wafer was cleaned by ultrasonic wave. In order to avoid the effect of diffusion, TaN with the thickness of 100 nm was deposited in between Cu and Si. The properties are shown in Table I. The thickness of Cu film was 1.5 μm measured with SEM.

3.2. Nanoindentation

The nanoindentation (NHT, CSM, Switzerland) was used. The load was fixed during the indention. The maximum load and depth were 30 mN and 0.75 μm respectively. Fig. 1 shows the typical load-depth curve of the nanoindentation.

The results of elastic modulus and hardness of Cu films are showed in Table II. The depth was controlled at about 150 nm in order to avoid the effect of the substrate.

TABLE I

Ultra-vacuum magnetron sputtering			Ion bean enhance deposition			
Sputtering power	Base pressure	Sputtering pressure (Ar)	Bombardment power	Current	Base pressure	Sputtering pressure (Ar)
200 W	5×10^{-5} Pa	1 Pa	600 eV	60 mA	3×10^{-3} Pa	0.1 Pa

TABLE II Elastic modulus and hardness of Cu film under different conditions

	−40 V	−60 V	−80 V	−100 V	20°C	100°C	200°C	300°C
Elastic modulus (GPa)	60.2	57.1	60.5	83.1	81.2	98.7	61.1	57.1
Hardness (GPa)	2.66	2.56	4.01	3.69	4.70	5.04	4.02	2.58

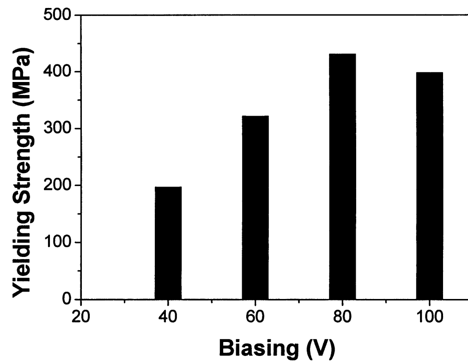

Figure 3 The yield strength of Cu thin film deposited with different bias.

4. Results and discussion

4.1. The effect of bias

Fig. 3 indicates that for magnetron sputtering technique the yield strength of Cu film increases with the increasing of bias. The maximum is 431 MPa and the minimum is 197 MPa. The result implies that the yield strength of thin film can be adjusted as bulk material.

The phase composition and texture of Cu films deposited with different bias were checked by X-ray diffraction (XRD). The crystal orientation was defined as diffraction intensity ratio of Cu-(111) and Cu-(200) planes. The results are shown in Fig. 4 and Table III.

Table III indicates that the ratio of diffraction intensity of Cu-(111) and Cu-(200) plane and the half width were affected by bias in deposition. Zhang and his coworkers [20] have pointed out that the orientation factor of grains, $C_{(\mathrm{hkl})} = \sin\varphi/(\cos\varphi\cos\lambda)$, and the grain size factor, $\mu_{\mathrm{f}}\ \mathrm{In}\ (d/b)/(d\sin\varphi)$, have strong effect on the yield strength of polycrystalline thin films. According their calculated data, for the orientation factor of grains in thin film with fcc lattice $C_{(200)} = 2.000$, and $C_{(111)} = 3.464$.

TABLE III The diffraction intensity ratio of Cu-(111) and Cu-(200) plane and the full width at half width of the diffraction peaks

Bias (V)	$I_{(111)}/I_{(200)}$	FWHM (111)	FWHM (200)
−40	2.53	0.28	0.24
−60	2.33	0.40	0.36
−80	4.13	0.44	0.48
−100	2.56	0.36	0.40

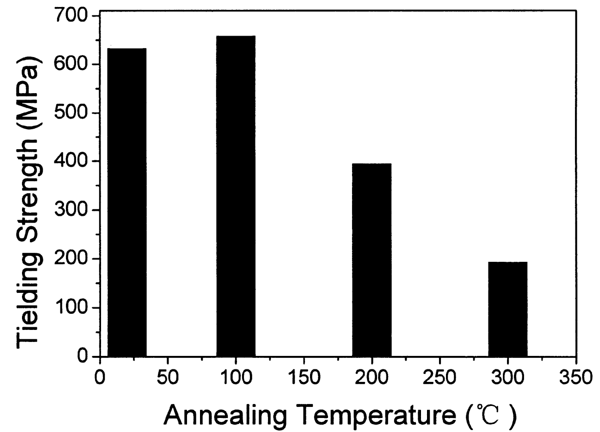

Figure 5 The yield strength of Cu film after annealed at different temperature.

It becomes recognizing that the changes of yield strength of thin film are directly proportional to the orientation factor of grains. The stronger is the (111) orientation or the less is the (200) orientation, the higher is the yield strength. As shown in Table III, the yield strength reaches the maximum as the diffraction intensity ratio of Cu-(111) to Cu-(200) was highest at the bias of −80 V. It is also known that the half width is related to grain size. From Table III, it could be seen that the width decreased with the increasing of bias and the yield strength reached the minimum at −80 V.

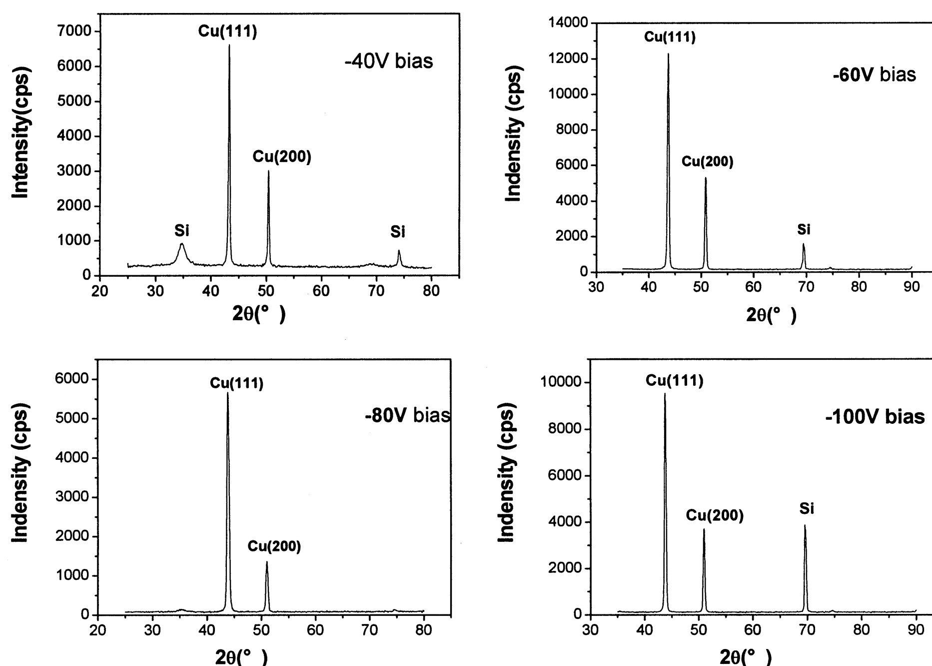

Figure 4 XRD spectrum of pure Cu films deposited with different bias.

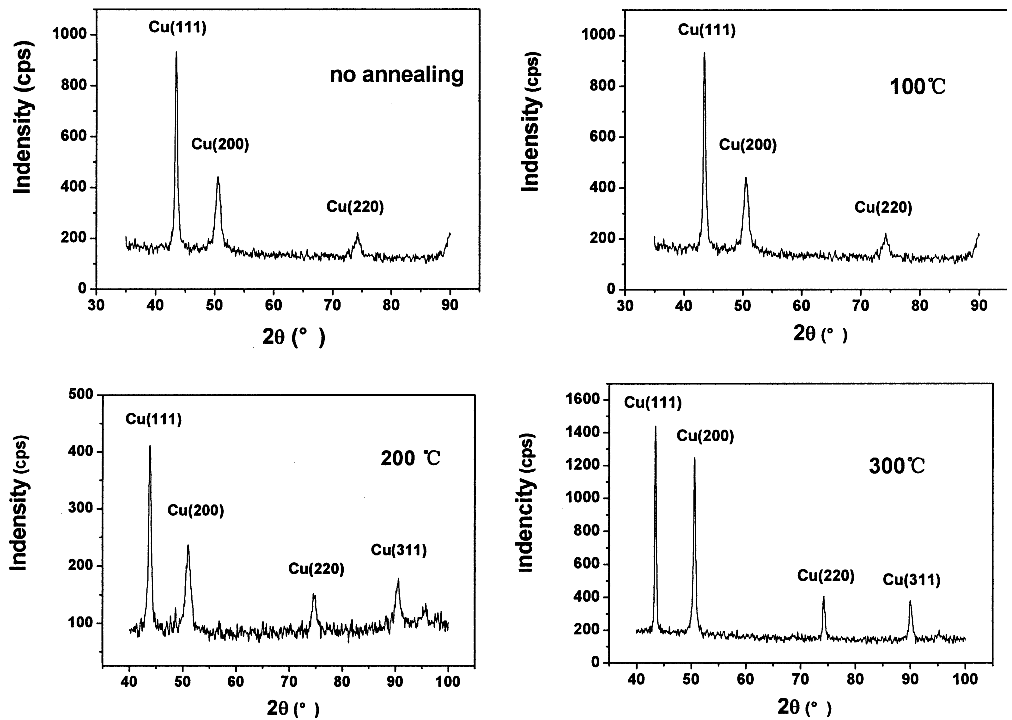

Figure 6 XRD spectrum of Cu films after annealed at different temperature.

From the above, it is easy to interpret the phenomena at −60 and −40 V. The intensities of Cu-(111) and Cu-(200) plane at −40 and −60 V were almost similar. But the grain size was smaller at −60 V, so the yield strength was higher. It was the same to the situation at the bias of −100 V. While the difference between −60 and −100 V might be caused by the structure or other changes. For example, the energy of bombardment ions could induce anti-deposition.

It is noted that the yield strength of Cu film deposited with different bias is far higher than that of bulk Cu (60–150 MPa). Zhang *et al.* proved analytically [19] that the yield strength decreases with the increasing of film thickness. Doemer [13], Li [18] and Venkatraman [20] showed that when the thickness of Al film was 0.2 μm, the yield strength could reach much high value of 400 MPa, while the yield strength was down to 200 MPa when the thickness was increased to 1 μm. In our research, the yield strength increased with increasing of bias, even though the thickness of films was almost identical.

4.2. The effect of annealing temperature

Fig. 5 shows the results of ion beam enhanced deposition. The maximum yield strength of as-deposited Cu film was 620 MPa, which is much higher than that of bulk Cu. When the post-annealing treatment was conducted, the yield strength would decrease as can be imagined, similar to the change of bulk material. It is interesting to note that the film still had high yield strength of 164 MPa even after it was annealed at 300°C. This is believed to be a result the constraint of the substrate. It must be bear in mind that the mechanical behavior of attached film differs greatly to that of free-standing film.

The XRD patterns are shown in Fig. 6 and Table IV. It can be seen that the Cu-(111) and Cu-(200) plane were two orientations for both as-deposited and annealed Cu films, but the relative intensity of the planes changed with the annealing temperature. When the annealing temperature was increased to 200 or 300°C, the yield strength decreased by 17.5 or 45.4% compared to that of as-deposited film, indicating that the orientation factor of crystals $C_{(hkl)}$ did affect the yield strength.

5. Conclusions

Through analyzing the loading process of nanoindentation with ideal and blunt Berkovich indenter by FEM, fitting exponent x of the load curve was obtained and the relationship between the maximum load P_m, the basic mechanical properties of film and substrate and the related r was also obtained. According to the above, the hardening index n_f and yield strength of thin film on ceramic substrate can be calculated by the load curve of nanoindentation.

TABLE IV The diffraction intensity of Cu-(111) and Cu-(200) plane and the half width of diffraction peaks

	As-deposited	Annealed at 100°C	Annealed at 200°C	Annealed at 300°C
$I_{(111)}/I_{(200)}$	2.106	2.326	1.737	1.149
FWHM (111)	0.440	0.440	0.400	0.360
FWHM (200)	1.680	1.840	1.640	0.480

Nanoindentation combining with finite element methods can be used to measure the yield strength of thin films. But the bluntness of the tip must be corrected. This method can reflect how the yield strength changes with the technological parameters. The experiments show that it is believable.

The biasing of magnetron sputtering can affect the crystal orientation and crystal size, and then affect the yield strength greatly. Under low biasing, with the increasing of biasing, the yield strength of Cu thin film increased.

The thick films can also have high yield strength as that of thin films by biasing deposition. The yield strength of Cu film has higher yield strength than that of bulk Cu. The annealing temperature affects the yield strength greatly. For the crystal orientation and grain size change a lot with the annealing temperature.

Acknowledgement

Thanks are due to Dr. Yuan Wang in Xi'an Jiaotong University for his assistance in film deposition. The financial supports of Natural Science Foundation of China (No. 59931010) and Foundation of State Ministry of Education for Skeleton Teachers are greatly appreciated.

References

1. D. T. REED and F. W. DALLY, *J. Mater. Res.* **8**(7) (1993) 1542.
2. J. A. RUUD, D. JOSELL and F. SPACPEN, *ibid.* **8**(7) (1993) 122.
3. A. J. GRIFFIN, JR., F. R. BROTZEN and C. F. DUNN, *Script. Metall.* **20**(9) (1986) 1271.
4. *Idem.*, *Thin Solid Films.* **150** (1987) 237.
5. G. MOULARD, G. CONTOUX, G. MOTYL, G. GARDET and M. COURBON, *J. Vac. Sci. Technol.* A **16**(2) (1998) 736.
6. E. WEPPELMANN and M. V. SWAIN, *Thin Solid Films.* **286** (1996) 111.
7. P. A. FLINN, D. S. GARDNER and W. D. NIX, *J. Mater. IEEE Trans. Electron Devices.* ED-**34**(3) (1987) 689.
8. M. D. TRAN, J. POUBLAN and J. H. DAUTZENBERG, *Thin Solid Films.* **308/309** (1997) 310.
9. P. A. FLINN, *J. Mater. Res.* **6**(7) (1991) 1498.
10. C. J. SHUTE and J. B. COHEN, *ibid.* **6**(5) (1991) 950.
11. J. B. PETHICA, R. HUTCHINGS and W. C. OLIVER, *Phil. Mag.* A **48** (1983) 593.
12. M. F. DOENER and W. D. NIX, *J. Mater. Res.* **1** (1986) 601.
13. M. F. DOERNER, D. S. GARDNER and W. D. NIX, *ibid.* **1** (1986) 845.
14. W. C. OLIVER and G. M. PHARR, *ibid.* **7** (1992) 1564.
15. D. J. MA, K. W. XU and J. W. HE, *Thin Solid Films.* **323** (1998) 183.
16. S. BADER, E. M. KALAUGHER and E. ARTZ, *ibid.* **263** (1995) 175.
17. C. J. SHUT and J. B. COHEN, *J. Mater. Res.* **1** (1991) 950.
18. Z. H. LI, G. Y. WU, Y. GU, W. R. CHEN and Y. Y. WANG, *J. Vac. Sci. Technol.* A **14** (1996) 2693.
19. P. A. FLINN, D. S. GARDNER and W. D. NIX, *J. Mater. IEEE Trans. Electron Devices.* ED-**34**(3) (1987) 689.
20. J. M. ZHANG and K. W. XU, *J. Ad. Mater.* **34**(1) (2002) 51.
21. R. VENKATRAMAN and J. C. BRAVMAN, *J. Mater. Res.* **7**(8) (1992) 2040.

Received 7 May 2003
and accepted 20 January 2004